Frequency and State-of-Charge Restoration Method in a Secondary Control of an Islanded Microgrid without Communication

Jin-Oh Lee [1] and **Yun-Su Kim** [2,*]

1   School of Electrical and Computer Engineering, Seoul National University, Seoul 08826, Korea;
    jolee0172@gmail.com
2   School of Integrated Technology, Gwangju Institute of Science and Technology (GIST), Gwangju 61005, Korea
*   Correspondence: yunsukim@gist.ac.kr

Featured Application: This work is applicable to a secondary control of distributed energy resources in a microgrid without using communication devices.

Abstract: This paper presents a control method for inverter-interfaced distributed generation (DG) and energy storage systems (ESSs) in an islanded microgrid. The proposed method is focused on secondary control, particularly frequency restoration and maintaining the ESSs' state of charge (SOC). To recover frequency deviation due to load change, an ESS is used as a droop-controlled grid-forming source. However, the grid-forming ESS cannot manage its own SOC, since it cannot control its own output power; hence, grid-feeding DGs are used to maintain the SOC within a desired range. Management of the SOC, as well as frequency restoration, is conducted by using local controllers without any communication devices, since dependency on communication may deteriorate system reliability in the case of failure. The proposed method for maintaining SOC can be realized by adjusting the system frequency, which is the only value that can be measured locally with almost the same value at every node in a steady state. Frequency restoration can be achieved by a simple ON/OFF scheme of the integral controller with a hysteresis loop to solve problems caused by differences between frequency measurements or set points among DGs.

1. Introduction

The growth of distributed generation (DG) systems has provided many solutions to local energy demand and supply problems. The concept of the microgrid was introduced in the early 2000s [1,2]. One important characteristic of the microgrid is that it can be isolated from or connected to the main power grid. During grid-connected mode operation, the microgrid voltage is maintained by the main grid, and in this mode, the main grid manages load changes in the microgrid with little impact on the system frequency, since the main grid has large inertia relative to the microgrid. In contrast, during islanded mode operation, the microgrid has small or zero mass moment of inertia (e.g., a microgrid with only inverter-interfaced units) [3–7]. Due to their weak inertia, islanded microgrids are vulnerable to load changes. Therefore, controllable distributed generators in an islanded microgrid must respond quickly to frequency deviation.

Energy storage systems (ESSs) have been widely used as primary control units for mitigating the effects of load changes, due to their fast-acting capability [8–11]. Primary control involves grid support and load sharing, which are usually achieved by droop control, and hence can be implemented locally

in a decentralized way. The conventional *P–f* droop control, virtual impedance loop-based control, adaptive droop control, and robust droop control are included in the droop control category as a primary control [12]. At the secondary control level, the state of charge (SOC) of ESSs and the frequency must be managed to operate an islanded microgrid securely. From the perspective of secondary control architecture, two approaches can be distinguished: centralized and decentralized [13]. Fully centralized control relies on a dedicated central controller with data-gathering capacity and extensive communication between the central controller and controlled units [13]. Hence, a fully centralized control method largely depends on a communication infrastructure that transfers all critical data for microgrid operation, and may limit system reliability in the case of communication failure. In particular, communication failures are more serious in islanded microgrids, since they are isolated from the main grid and must supply loads with limited resources. In contrast, in a fully decentralized control method, each unit only receives local data to operate the system and does not require full awareness of system-wide variables [14–16].

Most previous studies implemented a decentralized secondary control system using the multi-agent system (MAS) framework [17–22]. In reference [17], a secondary control method based on the MAS concept for microgrids is proposed as an alternative for the coordinated operation of microgrids. In reference [18], power flow calculations are performed to validate that the dispatched values from the market comply with the operational constraints. In [19], additional agents assigned to different tasks are shared by the DG units in proportion to their available unused capacity. A special case of MAS, i.e., a gossip-based technique, is proposed in [20]; here, different units exchange information regarding their operation, such as mismatches between programmed and actual power outputs, and marginal costs. In [21], additional agents that enable multi-stage operation scheduling of microgrids are included in a proposed architecture based on a MAS. A similar architecture, which considers demand-side bids and a sequential negotiation process, is proposed in [22]. Although MAS-based control strategies are largely based on agents' autonomy and performed locally, they are still based on a communication procedure. Technically, therefore, they are not fully decentralized and are still exposed to the risks of communication failure.

In reference [23], a wireless load-sharing controller for islanding parallel inverters in an AC-distributed system is proposed. The resistive output impedance of the parallel-connected inverters in an islanded microgrid is considered in the proposed controller. However, this does not take secondary control into account. In reference [24], a decentralized voltage control algorithm that minimizes power losses in a microgrid is proposed. Although the power losses are reduced using the proposed method, it does not consider SOC control of electric vehicles or the frequency of the microgrid. In reference [25], a control method for DG units to implement active power sharing and frequency recovery in an islanded microgrid is proposed. By using self-frequency recovery control, the frequency can be restored to the nominal value in a decentralized way. However, to offset the power-sharing mismatches among DGs after frequency recovery, communication is applied momentarily.

In reference [26], the distributed controllers for secondary frequency and voltage control in islanded microgrids is proposed. The proposed controller used local information and communication to perform secondary control. The authors mentioned that the communication between DGs has been a core ingredient in achieving the goal of the secondary control, which makes this paper more noticeable since the main contribution of this paper is to get rid of the communication on a secondary control level. In reference [27], the distributed cooperative control in an islanded microgrid secondary control is proposed. The authors used event-triggered strategy to reset the actual values in the feedback control schemes. The proposed method makes a profound contribution in terms of reducing communication dependency among DGs, but it still uses the communication in the secondary control level. In reference [28], the authors proposed the restoration control method of droop-controlled inverter-based microgrids. In reference [29], the authors used a distributed event-triggered secondary control method to deal with the economic dispatch and frequency restoration control for microgrids consisting of droop-controlled DGs. The authors of [30] and [31] also proposed distributed control

methods to restore the voltage and frequency deviation. Some distributed control methods are proposed to coordinate the secondary and tertiary control together [32–34]. However, all of them could not be performed in a communication-free manner.

In this paper, a fully decentralized control method for inverter-interfaced DGs, and an ESS without communication, are proposed. As reviewed in the previous works, the communication has been the most important but also the cost-inefficient ingredient in secondary control [26–29]. To the best of our knowledge, no literature has proposed a fully communication-free way in the secondary control of frequency and SOC restoration so far. In this context, this paper makes the major contribution of proposing a fully communication-free way of frequency and SOC restoration in the secondary control of islanded microgrids. Moreover, by introducing the communication-free secondary control for islanded microgrids for the first time, this paper can encourage many other future research projects on the secondary control of islanded microgrids without communication.

The proposed method assumed that all DGs and ESSs in an islanded microgrid have predetermined hourly output power set points, which are determined at the tertiary control level in accordance with the load pattern and economic benefits, so that the proposed method can be adapted more securely. Only the controllable DGs (i.e., diesel generator, fuel cell, biomass, etc.) are considered to adopt the proposed control method in this paper. The uncontrollable DGs such as renewable energy sources cannot or or partially (by using de-loaded control) able to adopt the proposed method. The proposed control method focuses on secondary control of DGs and the ESS. To ensure a rapid response to load changes, ESSs are used as droop-controlled grid-forming sources. When the SOC and/or frequency operating point deviates from the desired range, all grid-forming sources change their output frequencies. Grid-feeding DGs restore the frequency by changing their output power. To this end, we propose for grid-feeding DGs to use an integral control; however, if there are two or more units with integral control for frequency restoration, they conflict since the frequency measurements and/or the set points may differ from each other in the real world [25]. To prevent this problem, which is known as a hunting effect, an On/Off scheme for frequency integral controllers in grid-feeding DGs is also included in the proposed method, which is implemented to use local controllers and local information only without any communication devices to improve system reliability and reduce the installation cost. However, since this paper is focused on proposing the simple concept of the frequency recovery control without communication for the first time, the detailed analysis, such as stability analysis, has not been implemented. Hence, the scope of this paper is limited to the basic concept of the controller.

The rest of this paper is structured as follows. Section 2 briefly reviews conventional *P–f* droop control and introduces a droop coefficient determination method to synchronize the output powers of grid-forming units (ESSs in this paper), and hence permit other grid-forming units to estimate the SOC of the ESSs. Section 3 describes a method to integrate the SOC information into the frequency. Section 4 shows a controller for frequency restoration, Section 5 illustrates case studies verifying the effectiveness of the proposed methods, and Section 6 outlines the conclusions.

2. Sharing State-of-Charge (SOC) Information among Grid-Forming Units without Communication

To respond quickly to load changes, an ESS is proposed to be used as a grid-forming unit. Many studies have used ESSs as grid-feeding units for primary control [8–11], but a grid-forming unit reacts much faster than a grid-feeding unit and is able to share transient load changes, since a grid-forming unit is controlled as a voltage source [35]. By referring to [35], grid-forming control acts as a fixed-voltage source, and grid-feeding acts as a fixed-current source. For sharing a load change, conventional *P–f* droop control is used, and the relationship between the output active power and frequency of the grid-forming unit can be expressed as:

$$f_o = f_{nom} - m\left(P_o - P_{ref}\right) \qquad (1)$$

where f_{nom} and P_{ref} correspond to the nominal and reference values for frequency and output active power, respectively, and f_o and P_o correspond to the measured output frequency and active power, respectively. The coefficient m denotes the droop coefficient and is usually determined as [36]:

$$m = \frac{f_{nom} - f_{min}}{P_{max} - P_{min}} \tag{2}$$

where f_{min} is the allowable minimum value of the system frequency, and P_{max} and P_{min} are the maximum and minimum output power of a DG, respectively. f_{min} should be the same for all grid-forming units and P_{max} and P_{min} can be distinguished based on their power ratings and generation costs, etc. By adjusting the droop coefficients among grid-forming units, the proportion of load sharing can be determined as desired at the primary control level.

The main reason that ESSs have not been used as grid-forming units is that they cannot manage their own SOC, since a grid-forming type unit cannot control its own output power. To solve this problem, the output frequencies of all grid-forming units are adjusted to reflect the rough information of the SOC—i.e., whether the ESS should be charged or discharged—with respect to the frequency. To change the output frequencies of the grid-forming DGs almost simultaneously, other types of grid-forming DGs should know the SOC level of the grid-forming ESS. To achieve this without any communication devices at the secondary control level, it is assumed that all the hourly output power set points are predetermined, and the output power set point and droop coefficient of the ESS are given for every grid-forming DG. With those values known, other grid-forming DGs can estimate the output power of an ESS according to the following equations:

$$f_{o,ESS} = f_{nom} - m_{ESS}\left(P_{o,ESS} - P_{ref,ESS}\right) \tag{3}$$

$$f_{o,DG} = f_{nom} - m_{DG}\left(P_{o,DG} - P_{ref,DG}\right) \tag{4}$$

where the subscripts ESS and DG denote grid-forming ESS and another type of grid-forming DG, respectively. From the perspective of the ESS, m_{DG} and $P_{ref,DG}$ are given. Since $f_{o,DG}$ is identical to $f_{o,ESS}$, Equations (3) and (4) can be combined as:

$$m_{ESS}\left(P_{o,ESS} - P_{ref,ESS}\right) = m_{DG}\left(P_{o,DG} - P_{ref,DG}\right) \tag{5}$$

Equation (5) can be rearranged in terms of $P_{o,ESS}$ as:

$$P_{o,ESS} = \frac{m_{DG}}{m_{ESS}}\left(P_{o,DG} - P_{ref,DG}\right) + P_{ref,ESS} \tag{6}$$

From the perspective of grid-forming DG, all variables on the right-hand side of Equation (6) are known, so the output power of the grid-forming ESS can be calculated by Equation (6). The SOC of the grid-forming ESS can be expressed as [37]:

$$SOC_{ESS} = SOC_{ESS,init} - \int \frac{P_{o,ESS}}{CAP_{ESS}} dt \tag{7}$$

where SOC_{ESS} is the SOC of grid-forming ESS, $SOC_{ESS,init}$ is the initial value of SOC_{ESS}, and CAP_{ESS} is the capacity of the grid-forming ESS. Assuming that $SOC_{ESS,init}$ and CAP_{ESS} are known for every grid-forming DG, grid-forming DGs can estimate the SOC of the grid-forming ESS by using local parameters Equations (6) and (7), without any communication infrastructure.

In this way, all grid-forming units can share the SOC of the grid-forming ESS. It is important to share the SOC information among grid-forming units because this information is incorporated into the system frequency in the proposed method, and the system frequency can be adjusted only by grid-forming units. By measuring the system frequency locally, grid-feeding DGs can adjust their

output power to charge or discharge the ESS and hence maintain the SOC within a desired range. The details are discussed in the next section.

3. Reflection of SOC into the System Frequency

For the grid-feeding DG units to know the SOC of the ESSs based on the system frequency, the grid-forming units must change their output frequency with respect to the SOC. For grid-forming units to change their output frequency appropriately and allow grid-feeding units to support SOC and frequency management, all possible cases where the SOC needs to be supported must be investigated. The SOC has to be supported when it deviates from the allowable operation range, which is determined by the system operator; this situation is closely related to the output power of the ESS and the system load change, as shown in Table 1, where $P_{ESS,ref}$ and P_{ESS} are the reference power and output power of the ESS, respectively.

Table 1. All possible cases of state-of-charge (SOC) change.

| Case No.	Steady State	Transient State	After Load Change	
	Sign [1] of $P_{ESS,ref}$ (= Sign of P_{ESS})	Load Change	Sign [1] of P_{ESS}	Possible Risk
1		Increase	−	N/A
2			+	Low SOC
3	+	Decrease	−	High SOC
4			+	Low SOC
5		No change	−	N/A
6			+	Low SOC
7		Increase	−	High SOC
8			+	Low SOC
9	−	Decrease	−	High SOC
10			+	N/A
11		No change	−	High SOC
12			+	N/A

[1] Positive and negative signs for discharge and charge, respectively.

The sign of the ESS output power can be positive (discharging) or negative (charging). The case of zero output power is ignored because it does not cause any change in the SOC. It is assumed that, before the load change, the system is in a steady state and P_{ESS} is equal to $P_{ESS,ref}$. Hence, from Equation (1), the system frequency has a nominal value before the load change. In Table 1, Cases 1 and 10 never occur because the output power of the grid-forming ESS will not be increased/decreased after the load is decreased/increased. Similarly, Cases 5 and 12 occur neither since the sign of the output power will change without a load change.

In Cases 3 and 8, the status of the ESS is changed from charging/discharging to discharging/charging. In these cases, the discharging/charging status of the ESS causes a low/high SOC problem. A simple solution is to restore P_{ESS} to its reference value, so that the status of ESS can be changed again from discharging/charging to charging/discharging. This can be done by controlling grid-feeding units to recover the frequency to the nominal value (the details will be discussed in the next section).

However, there could be cases in which the frequency falls in the dead band range of the frequency support control of the grid-feeding units. Moreover, in the rest of the cases (Cases 2, 4, 6, 7, 9, and 11), frequency recovery cannot solve the low/high SOC problem since the sign of P_{ESS} is still the same as before the load change. In such cases, the output frequency of grid-forming DG must be changed by triggering the low/high SOC signal and hence allowing the grid-feeding DG units to measure the frequency deviation. By measuring the frequency deviation, grid-feeding DG units can adjust their power to restore the frequency and hence maintain the SOC (the details will be discussed in

the next section). To this end, a frequency reference controller for grid-forming DG is proposed as shown in Figure 1, where SOC_{min} and SOC_{max} are the allowable minimum and maximum of the SOC operation range determined by the operator, P_{res} is the active power reference during SOC restoration, P_{sched} is the hourly scheduled active power with respect to the system's load pattern, and m_{PF} is P–f droop coefficient.
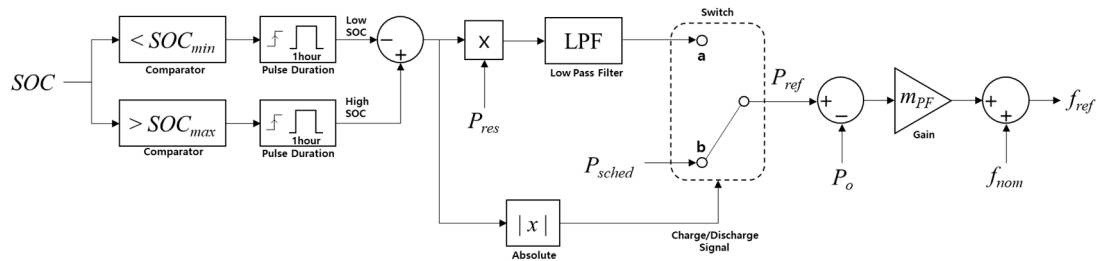
Figure 1. Proposed frequency reference controller for a droop-controlled grid-forming distributed generation (DG).

As shown in Figure 1, the SOC signal enters into the comparators, which check whether the SOC drops below SOC_{min} or exceeds SOC_{max}. If one of those events occurs, the output of the comparator triggers the pulse and generates '1' as the duration, which can be adjusted by the operator. Here, the duration is set as 1 h since the tertiary control time interval of P_{sched} is also considered as 1 h. This time interval can be adjusted by the operator. If P_{sched} is changed, the pulse (low/high SOC signal) is designed to be turned off so that the microgrid can be operated as scheduled data. Note that the output of the add/subtract component, '−1' (low SOC signal) or '+1' (high SOC signal) or '0', will be multiplied by P_{res}. Since the low/high SOC signal is a step signal, P_{res} multiplied by the low/high SOC signal enters into the low-pass filter (LPF) to alleviate any step change. Otherwise, a large step change of f_{ref} occurs and may result in instability of the system. The switch shown in Figure 1 chooses node 'a' or 'b' to provide an active power reference as low-pass filtered P_{res} or P_{sched}, respectively. The selection of the node is determined by the 'charging/discharging signal' shown at the bottom of Figure 1. Hence, P_{ref} can be expressed as:

$$P_{ref} = \begin{cases} P_{sched} & \text{, if Charge/Discharge signal is '0'} \\ P_{res,LPF} & \text{, if High SOC signal is '1'} \\ -P_{res,LPF} & \text{, if Low SOC signal is '1'} \end{cases} \tag{8}$$

where $P_{res,LPF}$ is the low-pass filtered P_{res}. The reason for predetermining P_{ref} as a specific constant value while the low/high SOC signal is turned on is that P_{ref} cannot be determined by some criterion considering the whole system. For instance, if communication is used, the charging/discharging active power reference can be determined by a central controller with consideration of the whole system. However, without communication, P_{ref} cannot be determined in a centralized way and hence should be determined locally. By only using local measurements and a local controller, it is impossible to calculate an optimal P_{ref}. Thus, for the sake of convenience, when the low/high SOC signal is turned on, P_{ref} is predetermined as a specific value. The rest of the control scheme is the same as with conventional P–f droop control [35,36]. The parameters used in Figure 1 are shown in Table 2.

Table 2. Parameters used in Figure 1.

SOC_{min} (%)	SOC_{max} (%)	Time Constant of Low Pass Filter (s)	Droop Coefficient, m_{PF} (pu)
20	90	0.0001	0.01

4. Frequency and SOC Restoration Control

As discussed in the previous section, if the SOC deviates from the allowable range, the system frequency is changed by adjusting P_{ref} of grid-forming DGs (see Figure 1), to restore the SOC within the allowable range. grid-feeding DGs adjust their output power by sensing the frequency deviation; thus, both the frequency and the SOC can be maintained within the desired range.

For a single grid-feeding DG, it may be too great a burden to undertake all frequency and SOC restorations. Hence, two or more grid-feeding DGs are proposed to support the frequency only with local measurements. To recover the frequency to the nominal value using only local measurements, integral control of frequency error must be applied. However, in the real world, local measurements and settings can differ slightly from each other, which may cause a problem while recovering the frequency [38]. For instance, two different frequency controllers will conflict with each other when recovering the frequency to the nominal value when their frequency measurements differ. To address this problem, communication is used for secondary control in the real world. To eliminate the dependency on communication, an active power controller for a grid-feeding DG is proposed, as shown in Figure 2, where Δf_{int} is a binary signal, '1' or '0', to control the "PI On/Off switch". If Δf_{int} is '1', the switch is connected to node 'a' and the error between f_{nom} and f_o enters into the PI controller. If Δf_{int} is '0', the switch is connected to node 'b' and the zero input enters into the PI controller. In other words, the PI controller acts as to eliminate the frequency deviation and yields a value to adjust the active power reference. Before adding this value to the active power reference, it passes the low-pass filter to prevent this value being changed in a step-wise way, and is added to P_{sched} to yield P_{ref}.
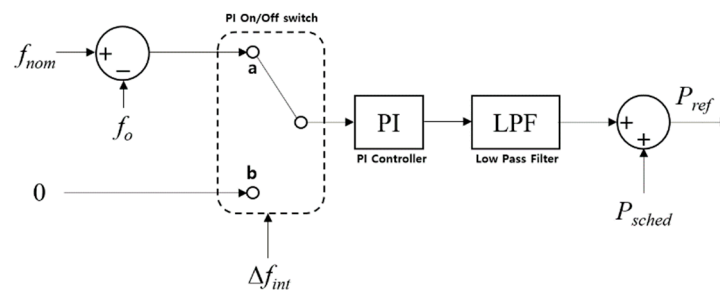
Figure 2. Proposed active power reference controller for grid-feeding distributed generation (DG).

The core part of the grid-feeding DG's active power controller is the process of generating the Δf_{int} signal, which is shown in Figure 3: the frequency deviation signal goes into the integrator through the dead band block, which prevents too-frequent activation of the Δf_{int} signal; hence, it tolerates a small deviation in the frequency. The absolute value of the integral of frequency deviation is compared to a certain constant value, K_{int}, to determine whether or not to restore the frequency. Note that the integrator is used to reflect not only the time, but also the magnitude of the frequency deviation. K_{int} can be adjusted by the system operator. By decreasing K_{int}, the frequency can be strictly adjusted to the nominal value but the output of the grid-feeding DG unit will be changed too frequently. The output of the comparator is multiplied by the output of the hysteresis loop, which yields '1' or '0'. Hence, Δf_{int} will be set to '1' to turn on the "PI On/Off switch" in Figure 2, only if both the comparator and the hysteresis loop outputs are '1' will the "PI on/off switch" be on; otherwise, it will be turned off. The hysteresis loop plays a key role in turning off the switch. It outputs '1' when the absolute value of the difference between f_{nom} and f_o exceeds a certain value, and outputs '0' if the frequency difference is restored back to a certain other value. For instance, if the former and the latter values are 0.1 and 0.01, respectively, the hysteresis loop outputs '1' if the absolute frequency difference exceeds 0.1 Hz, and outputs '0' if the absolute frequency difference is restored back to 0.01 Hz. Once the hysteresis loop outputs '0', Δf_{int} becomes '0' and the integrator is reset. Without the proposed hysteresis loop control, secondary control without communication cannot be implemented. The parameters used in Figures 2 and 3 are shown in Table 3.
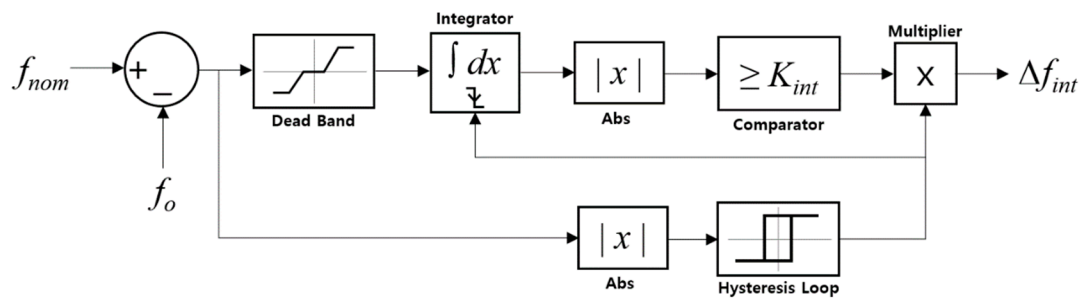
Figure 3. Proposed frequency deviation signal generator.

Table 3. Parameters used in Figures 2 and 3.

Proportional Gain (pu)	Integral Gain (pu)	Time Constant of LPF (s)	Dead Band Range (Hz)	K_{int} (Hz·s)	Hysteresis Loop ON/OFF Value (Hz)
0.00005	0.0006	0.03	± 0.1	50	0.1/0.01

In summary, the conventional droop control, which is one of the most widely used control methods, is used for the primary control in the proposed method. The proposed method is focused on the secondary control of restoring the frequency and the SOC. The methodology for this proposed control is just adding the active power reference changer for grid-forming unit as shown in Figure 1 and grid-feeding unit as shown in Figure 2 on to the conventional DG control schemes. The rate of active power reference change by the proposed part of the controller is small since we have added LPFs on them. Note that the change rate of the active power reference in the tertiary control is usually larger than that of the secondary control. However, it does not mean that the proposed method can perfectly guarantee the stability of the system. For precise analysis, the small-signal and large-signal stability have to be analyzed and all the parameters in Tables 2 and 3 should be reconsidered according to the stability analysis. Since the scope of this paper is limited to the basic concept of the controller, the stability analysis and mathematical proof remain as future works.

Consequently, the proposed part of the controller acts as a small-signal change in the conventional droop-based DGs. So, if the conventional droop-based control scheme is stable against a small signal, the proposed methodology can be regarded as stable system. The small-signal stability of microgrids with droop-based DGs has been researched in many other works in the literature and can be referred to [39–41].

5. Simulation Results and Discussion

5.1. Simulation Environment

The proposed method was tested by simulation to prove its effectiveness. The microgrid studied in [25], [42–44] was modeled with a slight modification and is shown in Figure 4. The power rating of all DGs (DG1 and DG3 are grid-forming units and DG2 and DG4 are grid-feeding units) in the microgrid is 2 MVA and the line parameters are shown in Figure 4. DG1 and DG3 are ESSs and both have a capacity of 4 MWh. Since it takes too long to see the change in SOC in the simulation, the capacity of ESS is scaled down to 1/3600 of 4 MWh. This means that the change in SOC in 1 h can be seen in 1 second (1/3600 h) of simulation time. The *P–f* droop coefficient for both DG1 and DG3 is 0.01, and the P_{sched} for all units is 0.4 MW.
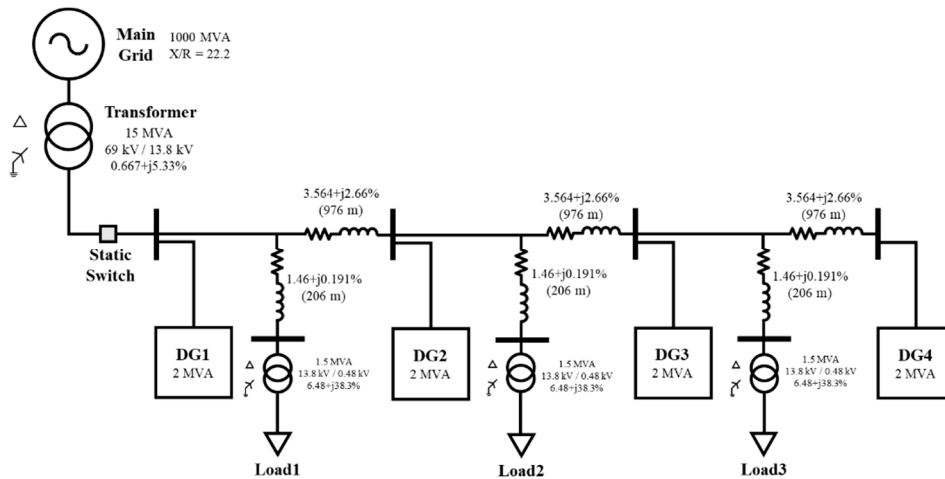
Figure 4. One-line diagram of the studied microgrid.

5.2. Case 1—Frequency Restoration

In Case 1, two different control methods for frequency restoration are compared. They adopt an integral controller and the proposed controller, respectively, for grid-feeding units for frequency restoration. The purpose of this case is to test whether the grid-feeding units restore the frequency without causing any problems, such as the hunting effect, while frequency measurement error among grid-feeding units is simulated. To simulate this measurement error, 0.001 Hz is added to the frequency measured by DG4. The load is changed after 0.8 s of the simulation to cause a frequency deviation. Figure 5 shows the simulation results achieved using an integral controller.
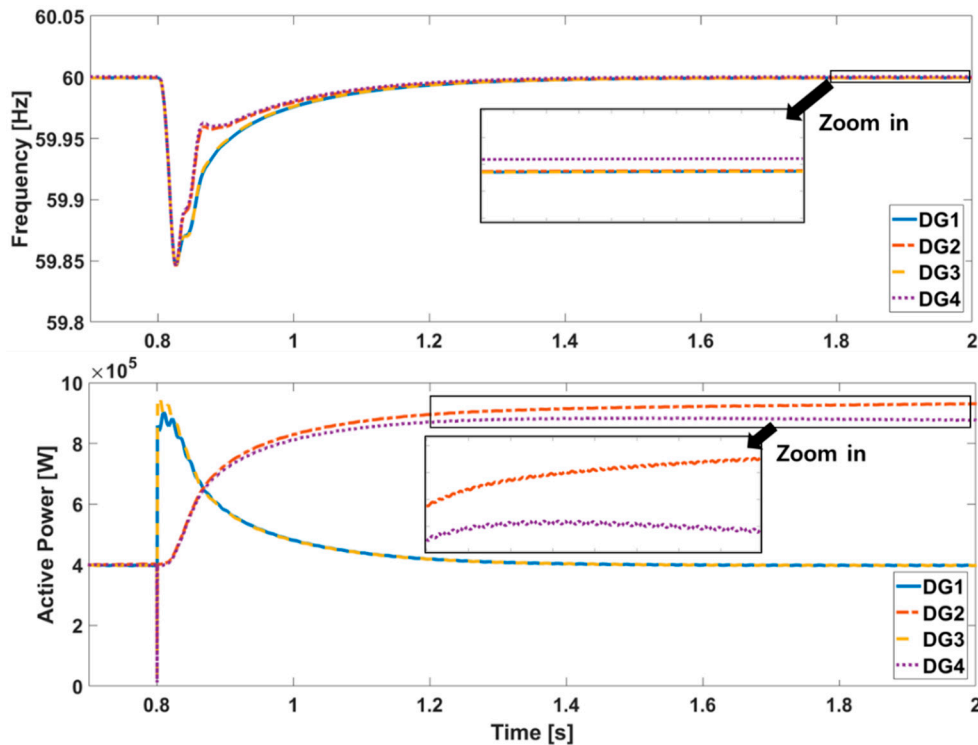

Figure 5. Frequency restoration results achieved using the integral controller.

As shown in Figure 5, the frequency drops at 0.8 s due to the load increment. Focusing closely on the zoom in part of the frequency, a measured frequency error among DGs can be observed. The active power of the grid-forming units immediately follows the load change at 0.8 s and hence changes their

output frequency. Since grid-feeding units adopt an integral controller to restore the frequency, their active power increases after frequency deviation. However, even after the frequency is restored back to nearly 60 Hz, the active power of DG2 and DG4 does not remain as the steady-state value, but is instead increased and decreased, respectively. This is due to the measurement error, which exists in the real world. Since DG2 and DG4 measure smaller and larger values than 60 Hz, respectively, they keep increasing and decreasing the active power, respectively. Eventually, the system will collapse. Furthermore, if there are set point errors in frequency reference and/or controller gain, the system frequency will not be maintained at a steady-state value.

To overcome this real world problem, new controllers are proposed and the simulation results obtained using the proposed controller are shown in Figure 6. After the frequency deviation, grid-feeding units wait for the Δf_{int} signal to restore the frequency. Slightly after 1.2 s of simulation time, the Δf_{int} of DG2 activates earlier than that of DG4, since DG2 measures a smaller frequency value than DG4. At 1.5 s, the Δf_{int} of DG4 is turned off earlier than that of DG2, since DG4 measures a larger frequency value than DG2. By using this control scheme, the active powers of DG2 and DG4 can reach the steady-state value (see the zoom in part of the active power in Figure 6), even if there is a frequency measurement error (see the zoom in part of the frequency in Figure 6).
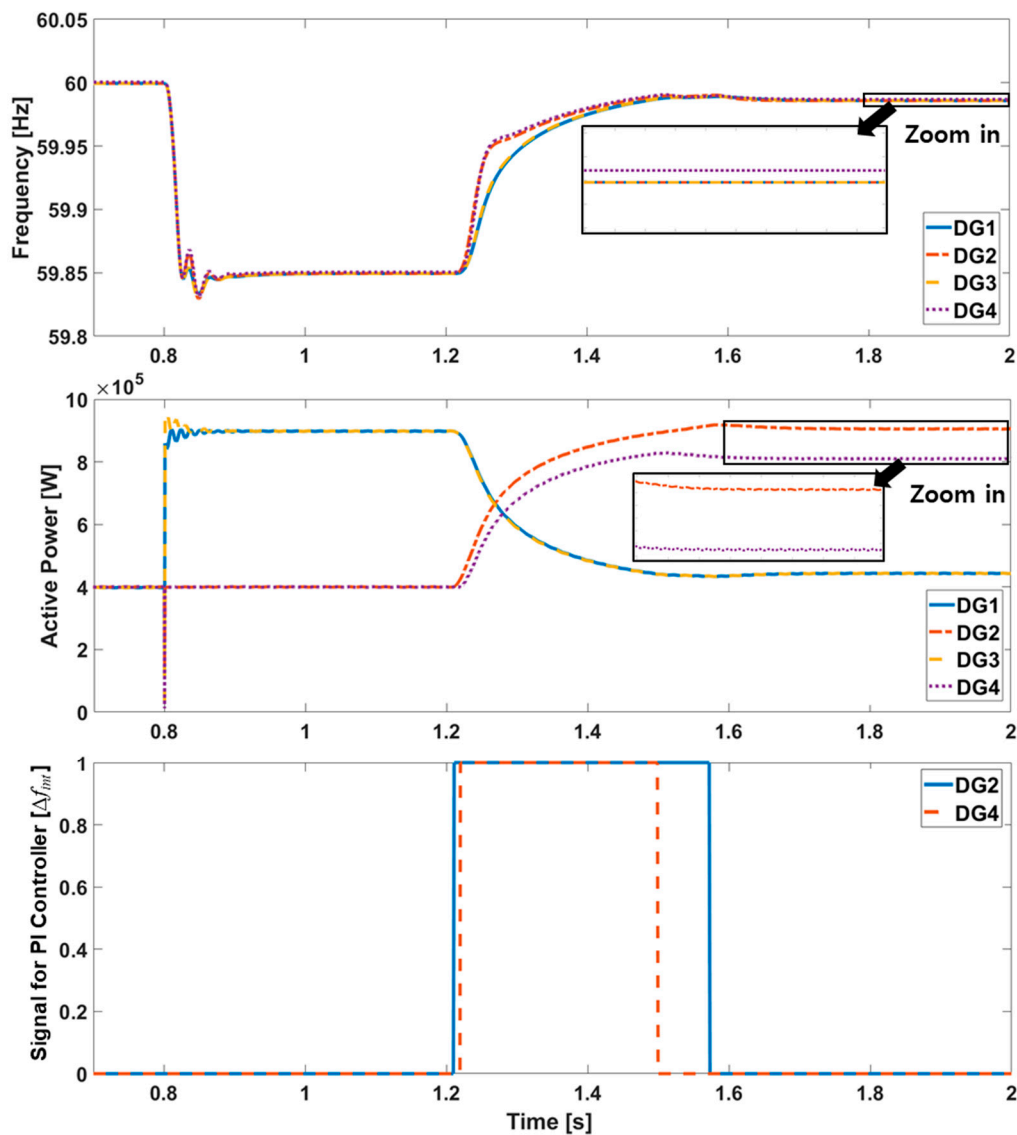

Figure 6. Frequency restoration results obtained using the proposed controller.

5.3. Case 2—SOC Restoration

This case shows that the proposed controller can be used to restore both the frequency and SOC without using communication. In this case, it is assumed that the SOCs of all grid-forming units are exactly the same.

As shown in Figure 7, the SOC drops below SOC_{min} (set as 20%) at 0.8 s. Subsequently, the low SOC signal (see Figure 1) is turned on and the grid-forming units change their P_{ref} to P_{res} (see Figure 1). Note that the active power of grid-forming units in Figure 7 did not change at 0.8 s. This means that there is no load change and the frequency is changed only to notify other grid-feeding units of the SOC shortage. After less than 0.2 s, the Δf_{int} of the grid-feeding units is turned on and the grid-feeding units start to restore the frequency by increasing their output. Simultaneously, by increasing the output of the grid-feeding units, the output of the grid-forming units becomes P_{res} (set as –0.5 MW) and the SOC is restored back to above SOC_{min}.
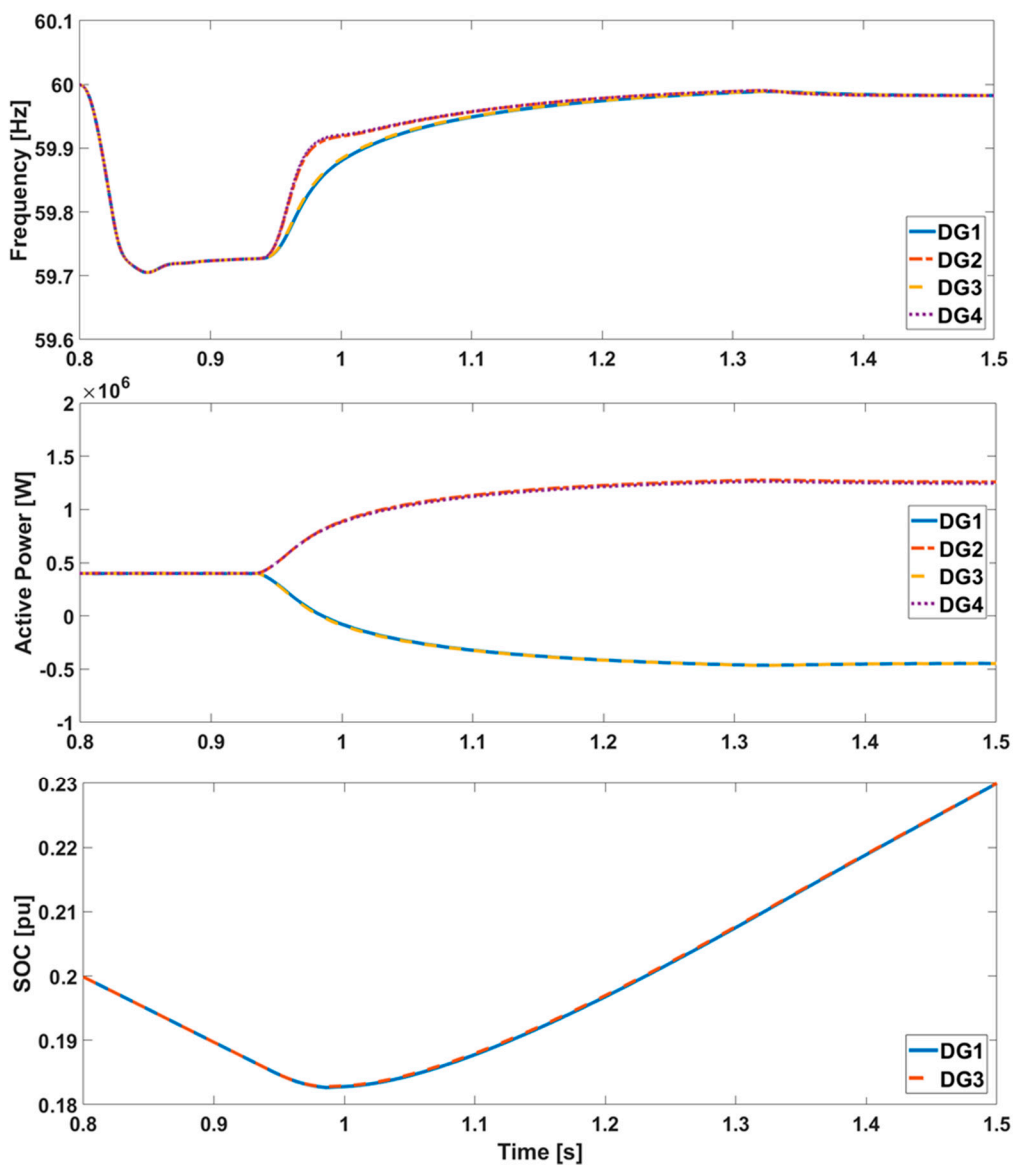

Figure 7. SOC restoration results when the SOCs are same.

5.4. Case 3—Existence of SOC Difference among Energy Storage Systems (ESSs)

Unlike Case 2, the SOC may not always be identical among ESSs. In Figure 8, simulation results are shown to illustrate the performance of the proposed controller while the SOCs differ among grid-forming units. Here, the SOC of DG3 is 1% larger than that of DG1. At 0.8 s, the SOC of DG1 drops below SOC_{min} (20%) and the output frequency drops due to the change in P_{ref}. However, the SOC of DG3 is still above SOC_{min} immediately after 0.8 s, and DG3 does not change its P_{ref}. Therefore, the two grid-forming units instantaneously output different frequencies. Since DG1 outputs a lower frequency than DG3 at 0.8–0.86 s, the output powers of DG1 and DG3 are decreased and increased, respectively. Consequently, the SOC of DG3 drops faster, and finally drops below 20%. At 0.99 s, Δf_{int} of the grid-feeding units is turned on and the frequency and SOC are restored.
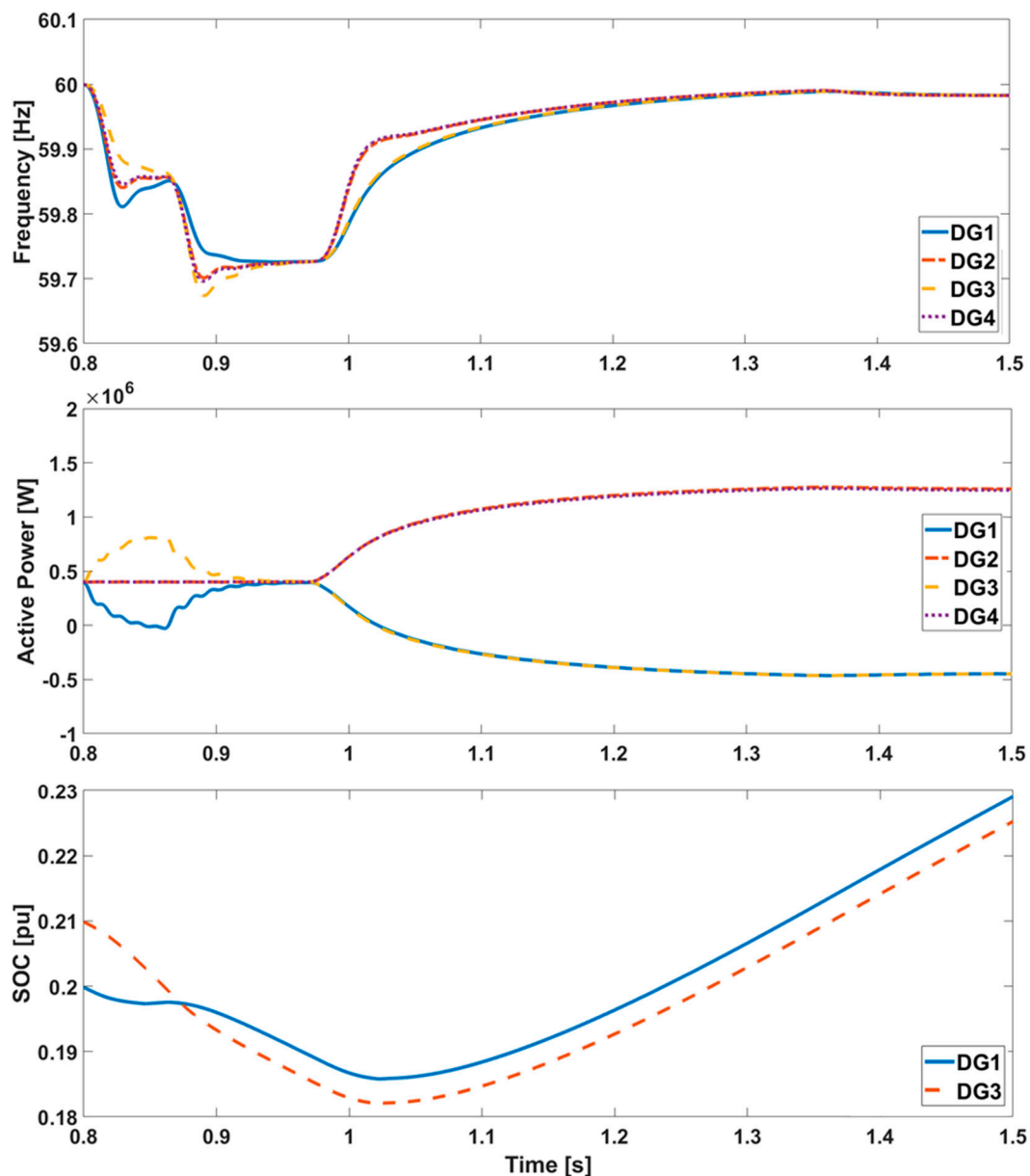

Figure 8. SOC restoration results for SOC difference of 1% between DG1 and DG3.

In Figure 9, simulation results of a larger SOC difference between DG1 and DG 3 are shown. Here, the SOC of DG3 is 5% larger than that of DG1 in order to prove the robustness of the proposed control method in for the worse situation. As shown in Figure 9, DG1 and DG3 deviated their output power

from the initial value in an opposite direction for a longer period than that of 1% SOC difference case in order to set their difference smaller. At 1.17 s, both SOCs are increased and thereby prove they worked as intended.
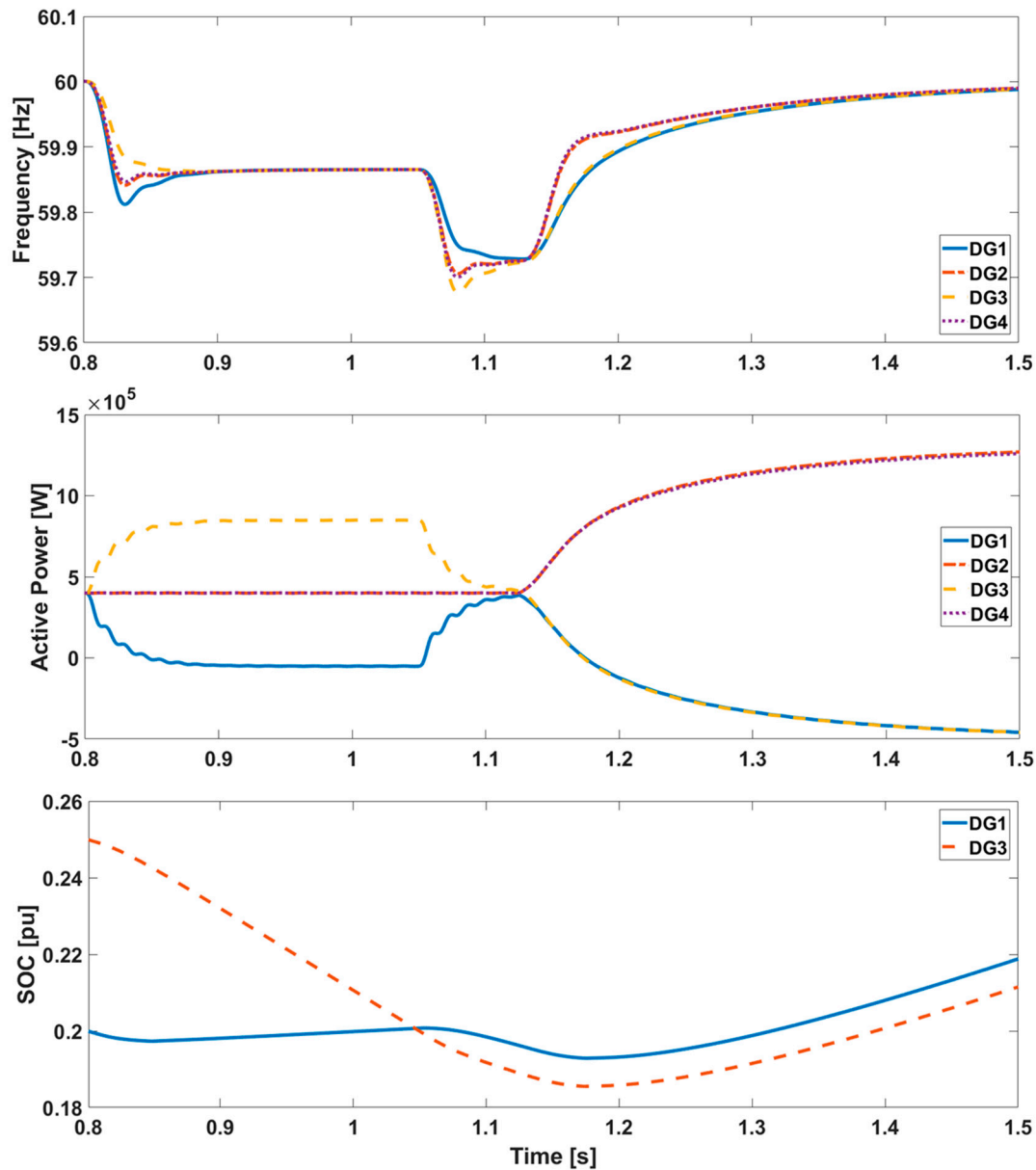

Figure 9. SOC restoration results for SOC difference of 5% between DG1 and DG3.

To show a more extreme case, even larger SOC difference among DG1 and DG3 is tested. In Figure 10, simulation results of 10% SOC difference among DG1 and DG 3 are shown. As shown in Figure 10, DG1 and DG3 deviated their output power from the initial value in an opposite direction for a longer period than that of the 5% SOC difference case in order to set their difference smaller. The cases of SOC difference of 1%, 5%, and 10% take 0.22 s, 0.37 s, and 0.56 s, respectively, to start to recover their SOCs within the allowable range. Interestingly enough, for all cases including Case 2 (zero SOC difference), the maximum SOC drop (the minimum SOC) is all the same in every case. It is slightly above 18%. From these simulation results, it can be concluded that the system can be stably operated even for a larger SOC difference among DGs.
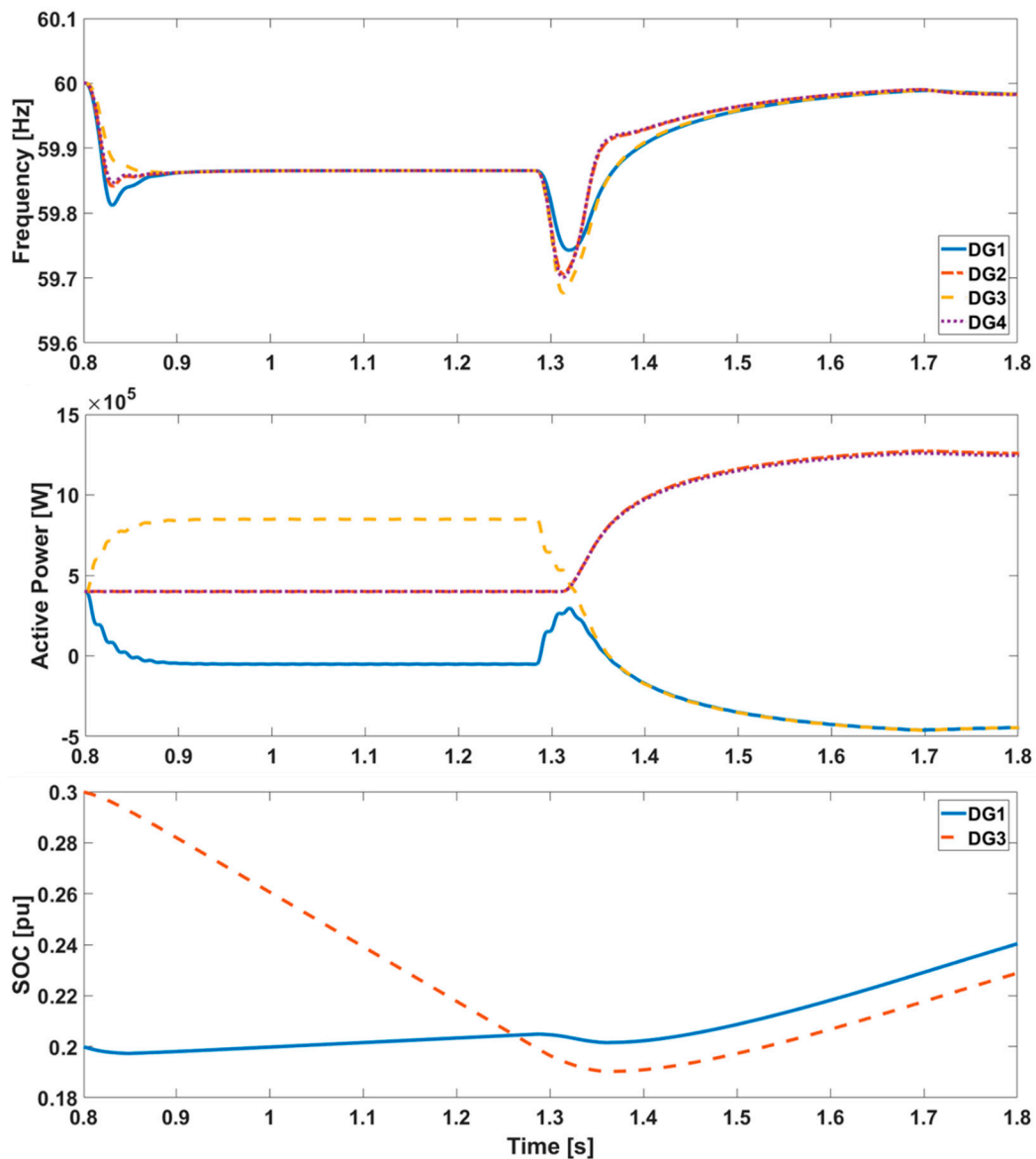
Figure 10. SOC restoration results for SOC difference of 10% between DG1 and DG3.

SOC difference larger than 10% can be regarded as a problem of SOC estimation and/or the tertiary control level and hence should be solved in terms of a different category. Otherwise, utilizing only a single ESS as the grid-forming unit could be one of the solutions for the SOC difference problem.

By conducting various simulations, the proposed controller is proved to be effective in many cases. However, it is worth noting that this paper is focused on the basic concept of the controller and hence the stability of the system should be further analyzed.

6. Conclusions and Future Works

The reliability of a microgrid is degraded by dependency on a communication system; however, due to problems such as the hunting effect, the frequency restoration process during secondary control of an islanded microgrid (or power system) relies on a communication system. To alleviate this dependency and hence enhance system reliability, new controllers are proposed for grid-forming and grid-feeding DGs in an inverter-based islanded microgrid. The performance of the proposed controllers focuses on the restoration of the frequency and the SOC without using communication.

The simulation is conducted by using MATLAB/SimPowerSystems and the results show that the proposed controller restores not only the frequency, but also the SOC by using only local controllers and data. Furthermore, no stability problems were identified, even with a frequency measurement error among DGs and the SOC difference up to 10% among grid-forming ESS units. From simulation results, it can be noted that an even larger SOC difference can be handled.

To achieve whole-system operation without communication, further control strategies must be developed. For instance, load shedding and reconnection schemes without communication are required to enhance system reliability. After developing such control strategies, others could also be developed step by step and a whole-operation procedure without communication could finally be realized. Furthermore, the stability analysis of the system should be studied in a future work to guarantee the reliability of the proposed controller.

To test the validity of the proposed method in a larger-scale microgrid also remains a future work. However, since the microgrid is usually a small-scale system consisting of several DGs, the scalability of the proposed methods is less important.

It is noticeable that the proposed method is focused on the secondary control only. To share the SOC information among grid-forming ESS units, it still needs some information from the tertiary control level where the communication is necessary. However, the tertiary control level needs a much lower frequency of information updates than the secondary control level. Hence, although it cannot abandon the communication infrastructure for the whole system control hierarchy, the dependency on communication is at least able to be alleviated by using the proposed control method.

Author Contributions: Investigation and methodology, J.-O.L.; conceptualization, supervision, project administration, and writing, Y.-S.K. All authors have read and agreed to the published version of the manuscript.

References

1. Lasseter, B. Microgrids [distributed power generation]. In Proceedings of the 2001 IEEE Power Engineering Society Winter Meeting, Columbus, OH, USA, 28 January–1 February 2001; pp. 146–149.
2. Lasseter, R.H. MicroGrids. In Proceedings of the 2002 IEEE Power Engineering Society Winter Meeting, New York, NY, USA, 27–31 January 2002; pp. 305–308.
3. Kim, Y.-S.; Kim, E.-S.; Moon, S.-I. Frequency and voltage control strategy of standalone microgrids with high penetration of intermittent renewable generation systems. *IEEE Trans. Power Syst.* **2016**, *31*, 718–728. [CrossRef]
4. Tang, X.; Hu, X.; Li, N.; Deng, W.; Zhang, G. A novel frequency and voltage control method for microgrid based on multienergy storages. *IEEE Trans. Smart Grid* **2016**, *7*, 410–419. [CrossRef]
5. Bose, U.; Chattopadhyay, S.K.; Chakraborty, C.; Pal, B. A novel method of frequency regulation in microgrid. *IEEE Trans. Ind. Appl.* **2019**, *55*, 111–121. [CrossRef]
6. Kerdphol, T.; Rahman, F.S.; Watanabe, M.; Mitani, Y. Robust virtual inertia control of a low inertia microgrid considering frequency measurement effects. *IEEE Access* **2019**, *7*, 57550–57560. [CrossRef]
7. Kerdphol, T.; Rahman, F.S.; Mitani, Y.; Watanabe, M.; Kufeoglu, S. Robust virtual inertial control of an islanded microgrid considering high penetration of renewable energy. *IEEE Access* **2018**, *6*, 625–636. [CrossRef]
8. Ribeiro, P.F.; Johnson, B.K.; Crow, M.L.; Arsoy, A.; Liu, Y. Energy storage systems for advanced power applications. *IEEE Proc.* **2001**, *89*, 1744–1756. [CrossRef]
9. Kim, J.-Y.; Jeon, J.; Kim, S.-K.; Cho, C.; Park, J.H.; Kim, H.-M.; Nam, K.-Y. Cooperative control strategy of energy storage system and microsources for stabilizing the microgrid during islanded operation. *IEEE Trans. Power Electron.* **2010**, *25*, 3037–3048.
10. Kong, X.-G.; Liu, Z.-Q.; Zhang, J.-H. New power management strategies for a microgrid with energy storage systems. *Energy Procedia* **2012**, *16*, 1678–1684.

11. Shim, J.W.; Verbic, G.; Zhang, N.; Hur, K. Harmonious integration of faster-acting energy storage systems into frequency control response in power grid with high renewable generation. *IEEE Trans. Power Syst.* **2018**, *33*, 6193–6205. [CrossRef]

12. Tayab, U.B.; Roslan, M.A.B.; Hwai, L.J.; Kashif, M. A review of droop control techniques for microgrid. *Renew. Sustain. Energy Rev.* **2017**, *76*, 717–727. [CrossRef]

13. Olivares, D.E.; Mehrizi-Sani, A.; Etemadi, A.; Canizares, C.; Iravani, M.; Kazerani, M.; Hajimiragha, A.H.; Gomis-Bellmunt, O.; Saeedifard, M.; Palma-Behnke, R.; et al. Trends in microgrid control. *IEEE Trans. Smart Grid* **2014**, *5*, 1905–1919. [CrossRef]

14. Ilic, M.D.; Liu, S.X. *Hierarchical Power Systems Control: Its Value in a Changing Industry (Advances in Industrial Control)*; Springer: London, UK, 1996.

15. Ilic-Spong, M.; Christensen, J.; Eichorn, K.L. Secondary voltage control using pilot point information. *IEEE Trans. Power Syst.* **1988**, *3*, 660–668. [CrossRef]

16. Ko, B.-S.; Lee, G.-Y.; Kim, S.-I.; Kim, R.-Y.; Cho, J.-T.; Kim, J.-Y. A positioning method of distributed power system by considering characteristics of droop control in a DC microgrid. *J. Electr. Eng. Technol.* **2018**, *13*, 620–630.

17. Dimeas, A.L.; Hatziargyriou, N.D. Operation of multiagent system for microgrid control. *IEEE Trans. Power Syst.* **2005**, *20*, 1447–1455. [CrossRef]

18. Logenthiran, T.; Srinivasan, D.; Wong, D. Multi-agent coordination for DER in microgrid. In Proceedings of the 2008 IEEE International Conference on Sustainable Energy Technologies, Singapore, Singapore, 24–27 November 2008; pp. 77–82.

19. Oyarzabal, J.; Jimeno, J.; Ruela, J.; Engler, A.; Hardt, C. Agent based micro grid management system. In Proceedings of the 2005 International Conference on Future Power Systems, Amsterdam, The Netherlands, 18 November 2005; pp. 6–11.

20. De Brabandere, K.; Vanthournout, K.; Driesen, J.; Deconinck, G.; Belmans, R. Control of microgrids. In Proceedings of the IEEE Power Engineering Society General Meeting, Tampa, FL, USA, 24–28 June 2007; pp. 1–7.

21. Zheng, W.-D.; Cai, J.-D. A multi-agent system for distributed energy resources control in microgrid. In Proceedings of the IEEE 5th Internation Conference on Critical Infrastructure, Beijing, China, 20–22 September 2010; pp. 1–5.

22. Logenthiran, T.; Srinivasan, D.; Khambadkone, A.; Aung, H. Multi-agent system (MAS) for short-term generation scheduling of a microgrid. In Proceedings of the IEEE Internation Conference on Sustainable Energy Technolog, Kandy, Sri Lanka, 6–9 December 2010; pp. 1–6.

23. Guerrero, J.M.; Matas, J.; de Vicuna, L.G.; Castilla, M.; Miret, J. Decentralized control for parallel operation of distributed generation inverters using resistive output impedance. *IEEE Trans. Ind. Electron.* **2007**, *54*, 994–1004. [CrossRef]

24. Ahn, C.; Peng, H. Decentralized voltage control to minimize distribution power loss of microgrids. *IEEE Trans. Smart Grid* **2013**, *4*, 1297–1304. [CrossRef]

25. Kim, Y.-S.; Kim, E.-S.; Moon, S.-I. Distributed generation control method for active power sharing and self-frequency recovery in an islanded microgrid. *IEEE Trans. Power Syst.* **2017**, *32*, 544–551. [CrossRef]

26. Simpson-Porco, J.W.; Shafiee, Q.; Dorfler, F.; Vasquez, J.C.; Guerrero, J.M.; Bullo, F. Secondary frequency and voltage control of islanded microgrids via distributed averaging. *IEEE Trans. Ind. Electron.* **2015**, *62*, 7025–7038. [CrossRef]

27. Chen, M.; Xiao, X.; Guerrero, J.M. Secondary restoration control of islanded microgrids with a decentralized event-triggered strategy. *IEEE Trans. Ind. Inform.* **2018**, *14*, 3870–3880. [CrossRef]

28. Guo, F.; Wen, C.; Mao, J.; Song, Y.-D. Distributed secondary voltage and frequency restoration control of droop-controlled inverter-based microgrids. *IEEE Trans. Ind. Electron.* **2015**, *62*, 4355–4364. [CrossRef]

29. Li, Z.; Cheng, Z.; Liang, J.J.; Si, J.; Dong, L.; Li, S. Distributed event-triggered secondary control for economic dispatch and frequency restoration control of droop-controlled AC microgrids. *IEEE Trans. Sustain. Energy* **2019**. [CrossRef]

30. Shafiee, Q.; Guerrero, J.M.; Vasquez, J.C. Distributed secondary control for islanded microgrids–A novel approach. *IEEE Trans. Power Electron.* **2014**, *29*, 1018–1031. [CrossRef]

31. Vasquez, N.; Yu, S.S.; Chau, T.K.; Fernando, T.; Iu, H.H.-C. A fully decentralized adaptive droop optimization strategy for power loss minimization in microgrids with PV-BESS. *IEEE Trans. Energy Convers.* **2019**, *34*, 385–395. [CrossRef]

32. De Azevedo, R.; Cintuglu, M.H.; Ma, T.; Mohammed, O.A. Multiagent-based optimal microgrid control using fully distributed diffusion strategy. *IEEE Trans. Smart Grid* **2017**, *8*, 1997–2008. [CrossRef]

33. Chen, G.; Lewis, F.L.; Feng, E.N.; Song, Y. Distributed optimal active power control of multiple generation systems. *IEEE Trans. Ind. Electron.* **2015**, *62*, 7079–7090. [CrossRef]

34. Wu, X.; Chen, L.; Shen, C.; Xu, Y.; He, J.; Fang, C. Distributed optimal operation of hierarchically controlled microgrids. *IET Gener. Transm. Ditrib.* **2018**, *12*, 4142–4252. [CrossRef]

35. Paquette, A.D.; Reno, M.J.; Harley, R.G.; Divan, D.M. Sharing transient loads: Causes of unequal transient load sharing in islanded microgrid operation. *IEEE Ind. Appl. Mag.* **2014**, *20*, 23–34. [CrossRef]

36. Lasseter, R.H.; Piagi, P. *Control and Design of Microgrid Components*; PSERC: Ithaca, NY, USA, 2006.

37. Kim, Y.-S.; Hwang, C.-S.; Kim, E.-S.; Cho, C. State of charge-based active power sharing method in a standalone microgrid with high penetration level of renewable energy sources. *Energies* **2016**, *9*, 480. [CrossRef]

38. Kundur, P. *Power System Stability and Control*; Mc-GrawHill: New York, NY, USA, 1994.

39. Dheer, D.K.; Kulkarni, O.V.; Doolla, S.; Rathore, A.K. Effect of reconfiguration and meshed networks on the small-signal stability margin of droop-based islanded microgrids. *IEEE Trans. Ind. Appl.* **2018**, *54*, 2821–2833. [CrossRef]

40. Wang, R.; Sun, Q.; Ma, D.; Liu, Z. The small-signal stability analysis of the droop-controlled converter in electromagnetic timescale. *IEEE Trans. Sustain. Energy* **2019**, *10*, 1459–1469. [CrossRef]

41. Li, Z.; Shahidehpour, M. Small-signal modeling and stability analysis of hybrid AC/DC microgrids. *IEEE Trans. Smart Grid* **2019**, *10*, 2080–2095. [CrossRef]

42. Ahn, S.-J.; Park, J.-W.; Chung, I.-Y.; Moon, S.-I.; Kang, S.-H.; Nam, S.-R. Power-sharing method of multiple distributed generators considering control modes and configurations of a microgrid. *IEEE Trans. Power Deliv.* **2010**, *25*, 2007–2016. [CrossRef]

43. Katiraei, F.; Iravani, M.R.; Lehn, P.W. Micro-grid autonomous operation during and subsequent to islanding process. *IEEE Trans. Power Deliv.* **2005**, *20*, 248–257. [CrossRef]

44. Katiraei, F.; Iravani, M.R. Power management strategies for a microgrid with multiple distributed generation units. *IEEE Trans. Power Syst.* **2006**, *21*, 1821–1831. [CrossRef]